

Modeling of the energy-loss piezoceramic resonators by electric equivalent networks with passive elements

Karlash V. L.

*S. P. Timoshenko Institute of Mechanics, The National Academy of Sciences of Ukraine
3 Nesterov str., 03057, Kyiv, Ukraine*

(Received 17 November 2014)

This paper is devoted to analysis of the modern achievements in energy loss problem for piezoceramic resonators. New experimental technique together with computing permits us to plot many resonators' parameters: admittance, impedance, phase angles, and power components etc. The author's opinion why mechanical quality under resonance is different from that under anti-resonance is given. The reason lies in clamped capacity and electromechanical coupling factor's value. The better electromechanical coupling, the stronger capacity clamping, and the higher its influence on anti-resonant frequency and quality. It is also established that considerable nonlinearity of admittance in constant voltage regime is caused by instantaneous power level.

Keywords: *piezoceramic resonators, electromechanical coupling, clamped capacity, instantaneous power*

2000 MSC: 74-05; 74F15

UDC: 534.121.1

1. Introduction

The energy loss problem is not a new problem for piezoelectrics. It appears in pioneer's works of the XX-th century beginning from W. G. Cady [1]; K. S. Van Dyke [2]; S. L. Quimby [3]; D. E. Dye [4], etc. Energy losses were accounted as viscosity, decaying decrements or acoustic radiation. Later W. P. Mason introduced an additive loss resistor into equivalent electric network [5]. In 60s and 70s, an idea of complex coefficients was suggested and back-grounded by S. E. Land et al. [6], G. Martin [7], R. Holland [8] etc. In present time, new piezoceramic materials with low losses and high electromechanical efficiency are created, and the loss problem for great power density conditions is unusual [9–11]. Now in analyze of energy losses they include three components: elastic, dielectric and piezoelectric ones [12–17]. The loss problem rises especially in high frequency (20–100 MHz) applications where the samples thickness reaches 200 mkm or less [18].

Elastic (mechanical) losses are explained as internal imperfections, such as internal friction, domain wall motion and lattice defects. Dielectric losses are caused by such imperfections which are connected with conductivity as well as lattice defects. At least, piezoelectric losses are coupled with imperfections of energy conversion process [12–17]. Analytic solutions for electroelastic vibrations of simple geometric form bodies such as bars, rods, disks, circular or cylindrical rings etc are known [13].

Imaginary parts usually are determined at maxima/minima admittance. This idea was first proposed by G. E. Martin for simple longitudinal vibrations of 1-dimensional thin piezoceramic rods and bars [7]. Many years ago, it was proposed to use thin piezoceramic disk's radial vibrations for such purpose, and corresponding formulae were derived [19,20]. Very important role in energy losses belongs to the mechanic quality factor Q , which differs for resonance and anti-resonance [21–23]. Usually in most cases, energy losses components are relatively small in comparison with real parts and may be represented in analytic solutions as imaginary parts of complex parameters [10–14].

Piezoceramic constructive elements' vibrations are characterized by great electromechanical coupling, elastic displacements, and stresses. In such bodies, the nature of the internal physical processes

leads to the fact that displacements, strains, stresses, admittance and impedance have both real and imaginary parts. It is possible to calculate any amplitude with taking into account the energy losses alone [14–17].

This paper is devoted to analysis of the modern achievements in energy loss problem for piezoceramic resonators. New experimental technique together with computing permits us to plot many resonators' parameters: admittance, impedance, phase angles, and power components etc. The author's opinion why mechanical quality is different at resonance and anti-resonance is given. The reason lies in clamped capacity and the value of electromechanical coupling factor. The better electromechanical coupling is, the stronger capacity clamping is, then the higher its influence on anti-resonant frequency and quality is. It is also established that considerable nonlinearity of admittance in constant voltage regime is caused by instantaneous power level.

2. Components of energy losses in piezoceramics and its influence on sample's full conductivity

Constructive elements made of piezoceramics have transversal isotropic symmetry of 6-mm class [13,14]. Their properties differ in polarization direction and in perpendicular directions a number of times. In analyses they are described by various elastic, dielectric and piezoelectric coefficients or moduli, which are represented mostly in complex form [12–17]

$$a = a_1 - ja_2 = a' - ja'' = a_{10}(1 - ja_{1m}); \frac{a_2}{a_1} = \frac{a''}{a'} = a_{1m} = \tan \xi. \quad (1)$$

Here in common view as a it is noted such electro-elastic coefficients as stiffness c_{ij} , compliances s_{kl} , piezomodulus d_{nm} , coupling factors k_{tr} , dielectric constants ε_{pq} etc. Expressions for elastic displacements U , strains ε and stresses σ , electric powers P , admittances Y or impedances Z , dimensionless frequencies x are complex too [16]. For imaginary parts of complex module were derived following restricting inequalities [12–14]

$$\begin{aligned} s''_{11}, s''_{33}, s''_{44}, s''_{66}, \varepsilon''_{11}, \varepsilon''_{33} \geq 0; \quad s''_{11} \geq |s''_{12}|; \quad s''_{11}s''_{33} \geq (s''_{13})^2; \quad s''_{11}\varepsilon''_{33} \geq (d''_{31})^2; \\ s''_{33}\varepsilon''_{33} \geq (d''_{33})^2; \quad s''_{33}(s''_{11} + s''_{12}) \geq 2(s''_{13})^2; \quad \varepsilon''_{33}(s''_{11} + s''_{12}) \geq 2(d''_{31})^2. \end{aligned} \quad (2)$$

All notations here and further were taken from [14–17]. These inequalities show that energy losses components in piezoelectric materials are not random but are coupled to each other. It means that having perfect elastic or dielectric properties, piezoelement has perfect electroelastic properties too. Values of loss tangent in modern piezoceramics lie in range 0.001 – 0.05.

Analytic calculations and experimental data show that losses influences vibrations are different at resonance / anti-resonance phenomena. Resonance amplitudes depend on elastic loss only – vibration's values inverse proportional to mechanical loss tangent s_{11m} (or direct proportional to mechanical quality Q_m). Anti-resonance amplitude depends on dielectric ε_{33m} , elastic s_{11m} and piezoelectric d_{31m} loss tangent together.

All modern methods of loss tangents determination base on maxima / minima admittance measure at first rod or bar mode of vibration. In principle this way may be used with any sample. As was shown in Ref [16] the piezoelectric resonator's admittance is inter-electrode capacity C_0 conductivity produced on anti-resonance $\Delta_a(x)$ to resonance $\Delta(x)$ determinants ratio

$$Y = j\omega C_0 \frac{\Delta_a(x)}{\Delta(x)}, \quad (3)$$

x is the dimensionless frequency, which depends on geometric sample's form.

The following formulae were derived for thin rod with thickness polarization, short cylindrical ring and high cylindrical shell with radial polarization accordingly [13,17]

$$Y_b = j\omega C_0 \left[1 - k_{31}^2 + \frac{k_{31}^2 \sin x}{x \cos x} \right] = j\omega C_0 \frac{\Delta_a(x)}{\Delta(x)}, \tag{4}$$

$$\Delta(x) = \cos(x), \quad \Delta_a(x) = (1 - k_{31}^2)\Delta(x) + k_{31}^2 \sin x/x,$$

$$Y_{sk} = j\omega C_0 \left[1 - k_{31}^2 + \frac{k_{31}^2 \omega_r^2}{\omega_r^2 - \omega^2} \right] = j\omega C_0 \frac{\Delta_a(x)}{\Delta(x)}, \tag{5}$$

$$\Delta(x) = \omega_r^2 - \omega^2, \quad \Delta_a(x) = (1 - k_{31}^2)\Delta(x) + k_{31}^2 \omega_r^2,$$

$$Y_{hk} = j\omega C_0 \left[1 - k_p^2 + \frac{(1 + \nu)k_p^2 \omega_r^2}{2(\omega_r^2 - \omega^2)} \right] = j\omega C_0 \frac{\Delta_a(x)}{\Delta(x)}, \tag{6}$$

$$\Delta(x) = \omega_r^2 - \omega^2, \quad \Delta_a(x) = (1 - k_p^2)\Delta(x) + (1 + \nu)k_p^2 \omega_r^2/2.$$

Here: j is the imaginary unit, ω is the angular frequency, ω_r is the resonant angular frequency, k_{31} is the transverse coupling coefficient, k_p is the planar coupling coefficient, ν is the Poisson ratio.

After substituting (1) in (4) and according to metamorphosis, G. E. Martin obtained approximate formulae for maxima Y_m and minima Y_n rod's admittances [7]

$$Y_m = \frac{8\omega_m C_0 k_{31}^2}{\pi^2 s_{11m}}, \quad Y_n = \omega_n C_0 \left[\varepsilon_{33m} - 2d_{31m} + \frac{\pi^2 s_{11m}}{8k_{31}^2} \right] \tag{7}$$

and

$$s_{11m} = \frac{16f_m C_0 k_{310}^2}{\pi Y_m}, \quad d_{31m} = \frac{\varepsilon_{33m}}{2} + \frac{\pi^2 s_{11m}}{16k_{310}^2} - \frac{Y_n}{4\pi f_n C_0}. \tag{8}$$

These expressions are used for loss components determination at present time too, and longitudinal thin rod's vibration is known now as a k_{31} mode [23]. Coupling coefficient is [7]

$$\frac{k_{310}^2}{1 - k_{310}^2} = \frac{\pi f_n}{2 f_m} \tan \left[\frac{(f_n - f_m)\pi}{2 f_m} \right]. \tag{9}$$

In a "short" cylindrical ring case, the dimensionless frequency is $x = \omega/\omega_r$ and

$$k_{310}^2 = \frac{\omega_a^2 - \omega_r^2}{\omega_a^2}, \tag{10}$$

which is known as Meson's formula [13]. Maxima admittance and mechanic quality are

$$Y_m = \omega_m C_0 k_{310}^2 Q_m = \frac{\omega_m C_0 k_{310}^2}{s_{11m}}, \quad Q_m = \frac{Y_m}{\omega_m C_0 k_{310}^2}. \tag{11}$$

In the "high" cylindrical ring case, the dimensionless frequency is $x = \omega/\omega_r$, and the coefficient k_p is determined from relation

$$\frac{2(1 - k_p^2)}{(1 + \nu)k_p^2} = \frac{f_m^2}{f_n^2 - f_m^2}. \tag{12}$$

Thin piezoceramic disk's radial vibrations have following admittance [14,15]

$$Y_{disk} = j\omega C_0 \left[1 - k_p^2 + \frac{(1 + \nu)k_p^2 J_1(x)}{\Delta(x)} \right] = j\omega C_0 \frac{\Delta_a(x)}{\Delta(x)}, \quad (13)$$

$$\Delta(x) = xJ_0(x) - (1 - \nu)J_1(x), \Delta_a(x) = (1 - k_p^2)\Delta(x) + (1 + \nu)k_p^2 J_1(x).$$

Dimensionless frequency for disk is $x = \omega R \sqrt{\rho s_{11}^E (1 - \nu^2)}$, where R is plate's radius, ρ is density.

After manipulating with complex functions in [14,15,19], and [20], it was obtained

$$s_{11m} \approx \frac{4.9 f_{m1} C_0 k_{po}^2}{Y_{m1}}, \quad d_{31m} \approx \frac{s_{11m} + \varepsilon_{33m}}{2} - \frac{Y_n}{4\pi f_{n1} C_0} + \frac{s_{11m} x_n \delta_n}{4\Delta_n} \quad (14)$$

$$\delta_n = (1 + k_{p0}^2)\beta_n + k_{p0}^2(1 + \nu)\gamma_n; \quad \gamma_n = [x_n J_0(x_n) - J_1(x_n)]/x_n;$$

$$\beta_n = (1 + \nu)J_0(x_n) - \kappa_0 J_1(x_n) - \Delta(x_n)/x_n, \quad \Delta_n = \Delta_a(x_n).$$

To use these formulae it is necessary to measure admittance maxima/minima and corresponding frequencies, and to calculate factors β , δ , γ at anti-resonance.

It is sufficient difference between constant current and constant voltage loading conditions for high power regime devices, such as radiators, ultrasonic motors or transformers.

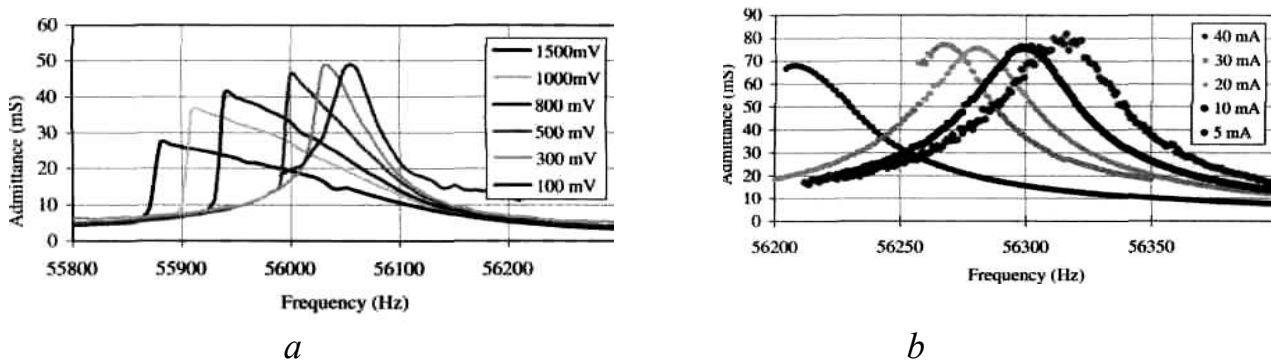


Fig. 1. Admittance dependences for constant voltage and constant current regimes [10].

Fig. 1, which is taken from C. O. Ural et al. article [10], shows that constant voltage regime is surrounded with great nonlinearity while constant current regime does not exhibit it. Data were obtained from longitudinal first mode rectangular PZT-8 plate vibration. Plate's size in paper [10] is absent. Authors consider that there is serious difficulty in determining the electromechanical coupling parameters under a high electric field drive from the admittance curves under a constant voltage condition. With a constant voltage method the resonance spectrum distorts significantly, sometimes exhibiting large hysteresis or a jump of the peak curve upon rising and falling frequency driving. This is caused mainly by the nonlinear elastic properties of the piezoceramics. Since, around the electromechanical resonance frequency, the vibration amplitude of a piezoelectric material is not proportional to the voltage, but to the current flowing through the sample. In order to determine the electromechanical coupling parameters precisely an admittance curve should be taken under a constant current condition. This method can determine the coupling parameters precisely from a perfectly symmetrical resonance spectrum, which is demonstrated in Fig. 1, b. However, using a constant current method, authors found that it can not be adapted to the anti-resonance mode characterization. This dilemma indicated the necessity of a new measurement system which can be used in a whole frequency range covering the resonance / anti-resonance.

Careful analyze of these graphs shows that maxima admittance for constant voltage conditions reach 50 mS only while at constant current it reach 80 mS. The maxima admittance frequencies lie in first case in range 55.9 – 56.1 kHz and in range 56.2 – 56.4 kHz for second case. It means that power and temperature conditions at constant voltage and constant current regime are not identical.

Simple calculations on Fig’s 1 data (Table 1, Table 2) show that constant voltage condition differs from constant current condition with maxima power level a number of times.

Table 1. Power’s maxima at constant voltage conditions for Fig’s 1 data.

U , mV	100	300	500	800	1000	1500
I , mA	4.9	14.7	29.5	33.6	37	40.5
P , mW	0.49	4.41	11.75	26.8	37	60.7

Table 2. Power’s maxima at constant current conditions for Fig’s 1 data.

I , mA	5	10	20	30	40
U , mV	71.5	131	266	400	558
P , mW	0.36	1.31	5.33	12	23.5

To examine the energy loss tangent’s influence on vibration characteristics the calculations were provided near maxima admittance/impedance for TsTBS-3 disk 66.4×3.1 mm. Formulae (13) were used in complex form (without Bessel function expansions) for dimensionless frequency ranges 2.05 – 2.1; 2.39 – 2.415 and $k_p^2 = 0.32$, $s_{11m} = 0.007$, $\epsilon_{33m} = 0.0085$. Piezoelectric loss tangent had three values: $d_{31m} = 0.0035$ (unbroken line on Fig. 2, *b*), 0.005 (dot curve) and 0.007 (broken line).

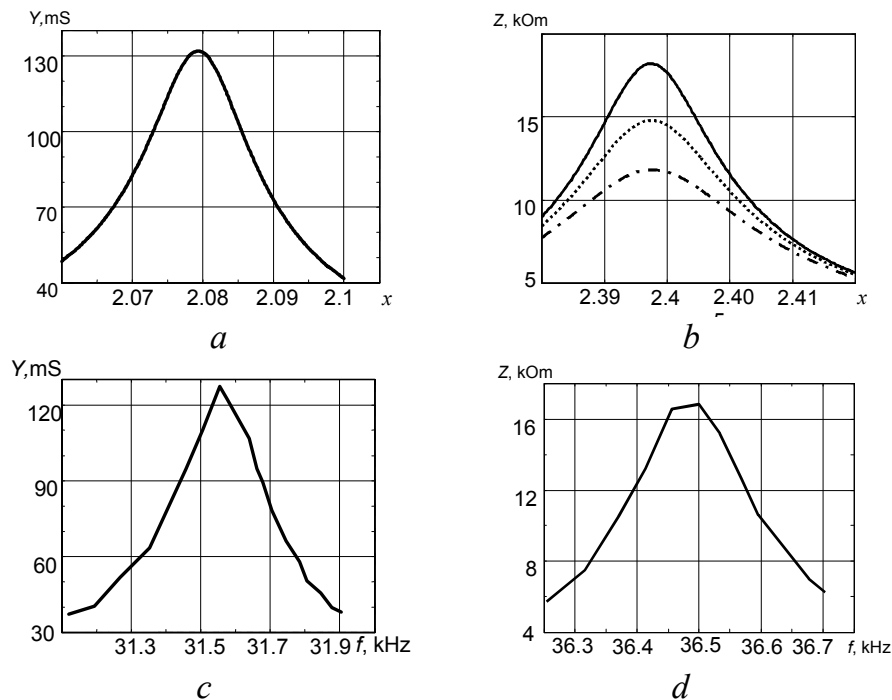


Fig. 2. Calculated and measured admittance-impedance dependences.

All three admittance curves (Fig. 2, *a*) coincide – dielectric and piezoelectric losses do not influence resonant vibrations near first resonance. On this graph there are obtained such values $Y_{m0} = 132$ mS, $Y_{1,2} = 93.3$ (on bandwidth ends – 3 dB level [10,21,23]), $x_0 = 2.079$, $Q_r = 138 – 148$. Impedance lines

(Fig. 2, *b*) differ in amplitude and have such bandwidth method determined qualities $Q_a = 228.4$; 184.5, and 171.4.

In experiment (Fig. 2, *c, d*) voltages are measured according to the modernized schema [16,24,25] and the following formula was used

$$Y_{pe} = \frac{I_{pe}}{U_{pe}} = \frac{U_R}{RU_{pe}}. \quad (15)$$

In parallel to output resistor $R2$ [26] there was included piezoelement Pe and loading resistors R . Voltmeter measured voltage U_{pe} dropped on piezoelement or voltage U_R dropped on loading resistors. Voltage U_R is proportional to electrical current I_{pe} in resistor and sample. The ratio of current to voltage is definite as admittance.

Loading resistor near resonance was 11.2 Ohm and near anti-resonance 20 kOhm. It was obtained $Y_m = 127.1$ mS, $Y_{-3db} = 89.87 \cong 90$ mS; $f_2 - f_1 = 22/28 * 300 = 235.7$ Hz; $Q_r = 31\ 551/235.7 = 138.8$; $Z_n = 16.86$ kOhm, $Z_{-3db} = 11.92$ kOhm; $f_2 - f_1 = 31/33 * 200 = 187.9$ Hz; $Q_a = 36.499/187.9 = 194.2$.

The results are in a good matching with calculated data and show that resonant and anti-resonant quality factors differ in almost 40% while in calculations there were taken the constant value for mechanical quality equal $Q_m = 143$. It means that conception of constant values of dielectric, elastic and piezoelectric loss tangent do not conflict with analytic and experimental results. Independence resonant phenomena upon dielectric and piezoelectric losses was postulated by G.W.Katz [27] for Rozen-type [28] transformer calculations and was used in my papers on this problem [29,30].

3. Experimental investigations

Many years ago and in modern time experimental research of energy losses in piezoelectric materials are based on measuring of the frequencies and admittances near resonance and anti-resonance. These frequencies are determined in analysis as that frequencies, where phase shifts between sample's voltage and its current are zero [13–17]. It is not lightly to reach such effect in practice, and resonant frequency f_r is identified with maxima admittance frequency f_m , while anti-resonant frequency f_a is identified with minima admittance frequency f_n . The fact is that the difference between $f_r - f_m$, as soon as $f_a - f_n$, is small and may be neglected for most cases.

The variants of simple experimental networks are well known and described in many Refs [13–15,26,27] etc. Such schemas are known as Meson's four-pole. Input voltage divider $R1$, $R2$ matches generator's output with measuring circuit and decreases ultrasonic generator's signal in $(R1 + R2)/R2$ times. In parallel to output resistor $R2$ is included piezoelement Pe and loading resistors R . Voltmeter in these schemas measures voltage U_R dropped on loading resistor, which is proportional to electrical current I_{pe} in resistor and sample. Voltage U_{pe} in this schema determined as difference between input voltage U_{in} and voltage U_R . Instead of exact formula (15) an approximate expression is used

$$Y_{pe1} = \frac{U_R}{R(U_{in} - U_R)}. \quad (16)$$

When loading resistor and sample change one another, the following approximate formula may be derived

$$Y_{pe2} = \frac{(U_{in} - U_{pe})}{RU_{pe}}. \quad (17)$$

As was shown in Refs [16,17,24,25] all three formulae give identical results on resonance and anti-resonance but it's differ strongly a far of these frequencies.

In contrast, the network, that presented in Refs [16,17,24,25], permits to measure with a great accuracy all voltages U_{pe} , U_{in} and U_R in a wide range around resonance and anti-resonance. This schema realizes three various loading conditions: 1) constant current, 2) constant sample's voltage, 3) con-

stant input voltage. Experimental data enter to PC and AFCh (amplitude-frequency characteristics) a number of physical parameters are plotted.

Formula (15) gives accurate data for all frequency range near resonances when $R = 3 - 15$ Ohm, and for anti-resonances it must be increased to $2 - 200$ kOhm. An influence of the loading resistor on obtained experimental data demonstrated Table 3. It shows that frequencies of admittance maxima have very small dependencies upon loading resistor value but strong for conductivity.

Table 3. Dependence of an admittance maxima and resonant frequency upon loading resistor's value

R , Ohm	1.6	5.3	11.2	230	993
f_r , kHz	31.572	31.560	31.562	31.563	31.576
Y_m , mS	131.4	124	119.6	101.4	26.36

Three measured voltages U_{pe} , U_R and U_{in} create peculiar characteristic triangle and angles between its sides may be calculated with using a cosine law as

$$\cos \alpha = \frac{U_{pe}^2 + U_R^2 - U_{in}^2}{2U_{pe}U_R}, \quad \cos \beta = \frac{U_{in}^2 + U_R^2 - U_{pe}^2}{2U_{in}U_R}, \quad \cos \gamma = \frac{U_{in}^2 + U_{pe}^2 - U_R^2}{2U_{in}U_{pe}}. \quad (18)$$

AFCh of an admittance near resonances and of an impedance near anti-resonance were plotted and used for determinations of Q_a and Q_b quality on -3 dB bandwidths method [9,10,16,17,23].

4. Equivalent electrical circuit of a piezoelement for low and high powers

In our time for commercial purpose various type piezoelectric bodies are made and used [9–17,23]. Modes of vibration differ too: longitudinal, flexural or shear for low frequencies; lateral and radial for middle frequencies and thickness for high frequencies. It is very difficult to make the element thinner 0.1 mm [26]. Single equivalent electrical network can't to satisfy all these damages and various variants such circuits were proposed. First schemas were described by W. G. Cady [1], K. S. Van Dyke [2], S. L. Quimby [3] and D. E. Dye [4]. All listed works had very interest results and outstripped the time. For example, W. G. Cady [1] in 1922 investigated thin narrow quartz rod longitudinal vibrations and found that electromechanical efficiency reaches maxima for the case, when electrode covers place's surface partly, on 75% D. E. Dye [4] studied such rod with divided electrodes and observed smoldering discharge. It was a first piesotransformer, but researcher doesn't understand that fact. Rozen-type piezotransformer [28] was patented through 30 years! Most known is Van Dyke schema with two capacitors and inductance. W. Mason refined it for Rochelle salt [5]. B. Van der Veen [31] proposed the equivalent network for thin piezoelectric rod with divided electrodes longitudinal vibration. E. C. Munk proposed an equivalent electrical circuit for radial modes of a piezoelectric ceramic disk with concentric (divided) electrodes [32]. A. V. Mezheritsky [18] proposed a number of equivalent circuits for a high-frequency, high-capacitance piezoceramic resonator with resistive electrodes.

Four variants of classic Van Dyke-type equivalent circuit are demonstrated on Fig. 3.

Vibrating system for any piezoelectric resonator may be presented an equivalent electrical network (Fig. 3, *a, b*), in which in parallel to static inter-electrode capacity C_0 is connected a series branch, consisting from inductance L , capacitor C and resistor r (this resistor symbolizes elastic energy losses). Such system is called with third view circuit [33]. A voltage resonance in series circuit corresponds to resonant frequency when $r = 1/Y_m$. And the current resonance in parallel circuit corresponds to anti-resonant frequency. This parallel circuit consists from inductance L and equivalent condenser C' , which created by C_0 and C in series $C' = C_0C/(C_0 + C)$.

In radio-engineering quality Q of resonant system determined as ratio of stored in circuit energy E_{stor} to loss energy $E_{dis.av}$ which dissipate during vibration period. It expressed with circuit parameters

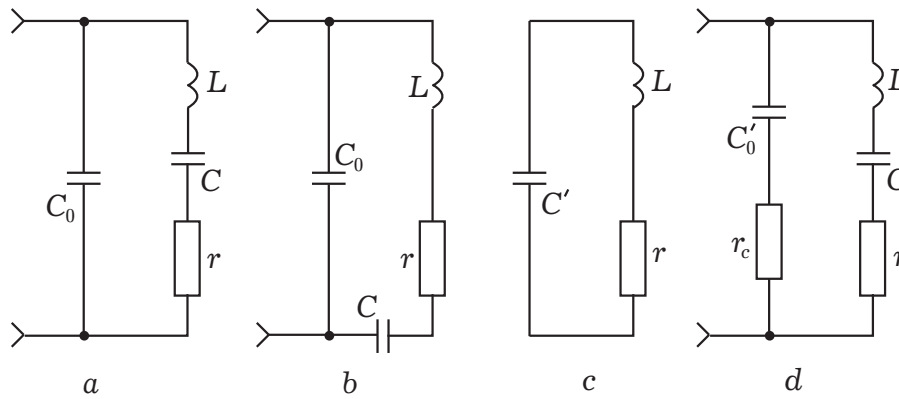


Fig. 3. Variants of Van Dyke-type equivalent circuit.

in such a way [33,34]

$$Q = 2\pi \frac{E_{stor}}{E_{dis.av}} = \frac{\rho}{r} = \frac{2\pi f_0 L}{r} = \frac{1}{2\pi f C}, \quad \rho = \sqrt{\frac{L}{C}}, \quad f_0 = \frac{1}{2\pi\sqrt{LC}}, \quad (19)$$

ρ is wave circuit resistance, r is loss resistor, f_0 is resonant frequency, L and C are circuit inductance and capacity.

The following formulae may be obtained for equivalent capacity and inductance

$$C = \frac{1}{\rho\omega} = \frac{1}{2\pi f_0 \rho} = \frac{1}{2\pi f_0 Q_r r}, \quad L = \frac{\rho}{\omega} = \frac{\rho}{2\pi f_0} = \frac{Q_r r}{2\pi f_0}. \quad (20)$$

In our disk $66.4 * 3.1$ mm, loading on 11.2 Ohm, loss resistor was $r = 7.87$ Ohm, $Q_r = 138.8$ and $\rho = Q_r * r = 1092$ Ohm, $f_0 = 3.155 * 10^4$, $C_0 = 1.849 * 10^{-8}$ F. Substituting these data in (20) we may obtain $C = 1/(2 * 3.14 * 1.092 * 3.155 * 10^7)$ F = $1/(2.164 * 10^8)$ F = $4.62 * 10^{-9}$ F, $L = 1092/(2 * 3.14 * 3.155 * 10^4) = 5.51 * 10^{-3}$ Hn. Parallel circuit capacity is $C' = C * C_0/(C + C_0) = 4.62 * 18.49/(4.62 + 18.49) * 10^{-9}$ F = $3.696 * 10^{-9}$ F. Parallel resonance frequency, wave resistance and anti-resonant quality factor are $f_n = 3.528 * 10^4$ Hz, $\rho = 1221$ Ohm, $Q_a = 1221/7.87 = 155.1$. Measured values were about 36499 Hz, $Q_a = 194.2$.

Why so great discrepancy between calculated and measured values of qualities and anti-resonant frequencies exists? The reason lies in clamped capacity and electromechanical coupling factor's values. The better electromechanical coupling the stronger capacity clamping and the higher its influence on anti-resonant frequency and quality. In our disk case $k_p^2 = 0.32$ and $C_{0c} = (1 - k_p^2)C_0 = 0.68 * 1.849 * 10^{-8}$ F = $1.257 * 10^{-8}$ F. After such correction we have $C'_1 = 4.62 * 12.57/(4.62 + 12.57) * 10^{-9}$ F = $3.378 * 10^{-9}$ F, $f_n = 3.69 * 10^4$ Hz, $\rho = 1277$ Ohm, $Q_a = 1277/7.87 = 162.3$. Frequency difference now is 0.9 %, quality difference – 16.4 %.

Fig. 4 presents a result of modeling equivalent network with passive elements. For equivalent electric schema, consisting from L , C , R elements such as 0.4 mHn, 1.814 nF and 9.579 nF, were made voltage measurements with loading resistor 11.2 Ohm. Constant current and constant voltage conditions were used. Graphs are plotted for voltages, input admittance, cosines, angles and real / imaginary admittance components. Graphs are obtained for constant current $I_{eq} = U_R/R = 15$ mV/ 11.2 Ohm = 1.34 mA (left), constant voltage $U_{eq} = 60$ mV (centre) and constant input voltage $U_{in} = 100$ mV (right) conditions near series circuit resonance. For model's case voltage U_{eq} is identical to voltage U_{pe} for sample, and current I_{eq} is identical to current I_{pe} for sample.

On higher graphs (first row) U_{eq} are shown as broken curves, U_{in} – as dot curves and U_R as unbroken lines. Full admittances (second row) are calculated with formulae (15) (unbroken lines), (16) (dot lines) and (17) (broken curves). Third and forth rows present cosines of triangle's angles and corresponding angles. Angle α (dot lines) is created by U_R and U_{eq} sides. It characterizes a phase shift

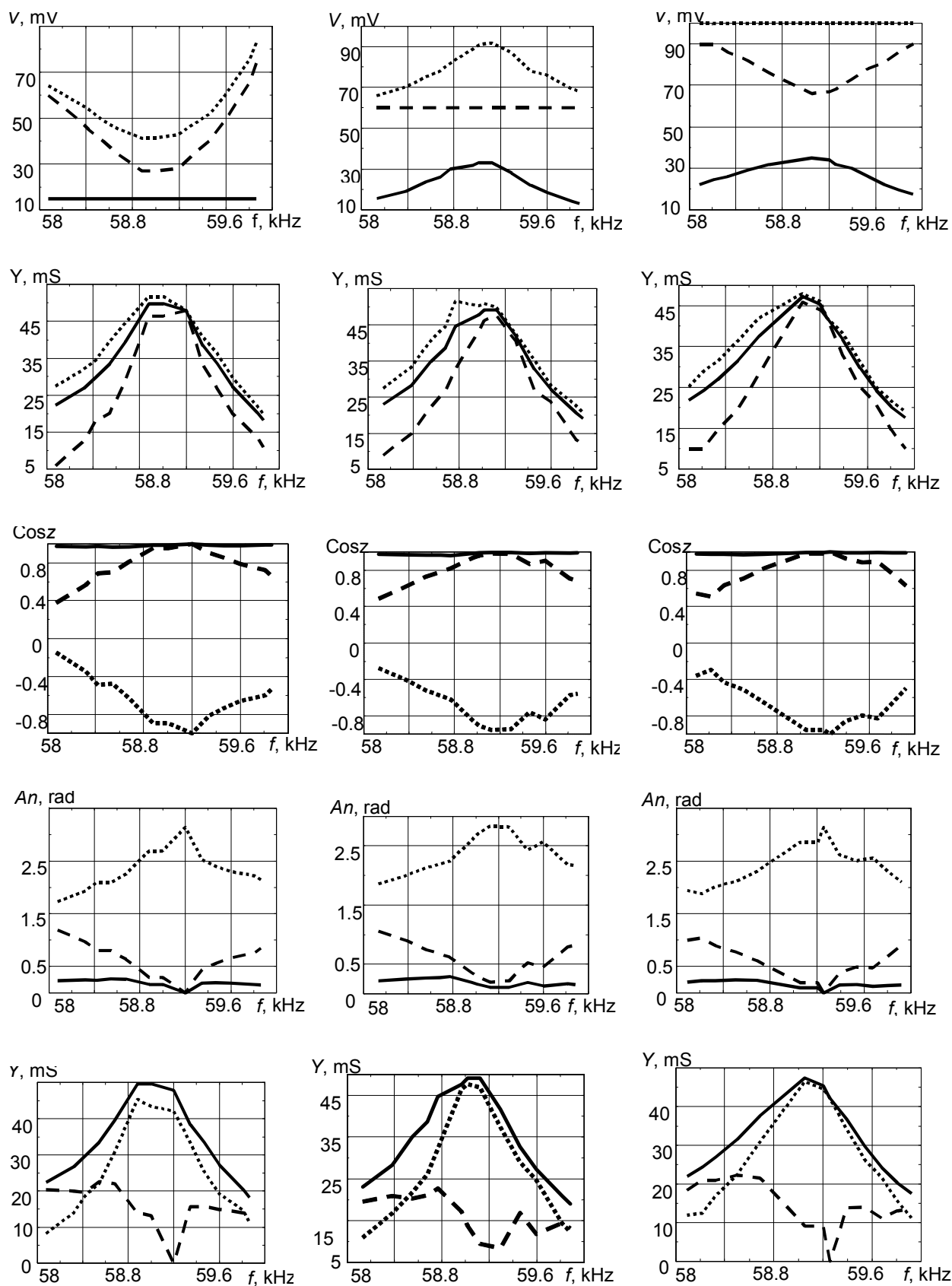


Fig. 4. Result of modeling equivalent network with passive elements.

between circuit's current and voltage. Angle β (broken curves) is created by sides U_{in} and U_R . It is according to phase shift between output generator voltage and consuming current. At least, angle γ (unbroken lines) is created by sides U_{in} and U_{eq} , i.e. between output generator voltage and equivalent circuit's voltage. Lower, fifth row presents full Y (unbroken curves), real G (dot lines) and imaginary B (broken curves) parts of circuit admittance, calculated with formulae

$$G_1 = Y_{pe} \cos \beta, \quad B_1 = Y_{pe} \sin \beta; \quad (21)$$

or

$$G_2 = Y_{pe} / \sqrt{1 + k^2}, \quad B_2 = G_2 k, \quad k = \tan \beta. \quad (22)$$

Both expressions gave same results and serve here for compare.

In general, graphs of Fig.4 are similar to that of real sample [16] and show that for small signal appropriate circumstances constant current and constant voltage regimes exhibit same result.

Table 4. Shunting capacity influence on equivalent network parameters.

C_0 , nF	6.716	10.5	36.1	70.44	36.1 + R1	36.1 + R2
f_r , kHz	59.23	59.09	58.92	58.61	58.95	58.69
f_{a1} , kHz	66.63	64.3	60.53	59.83	60.88	60.59
f_{a2} , kHz	66.73	64.3	60.39	59.32	60.39	60.39
L , mHn	3.99	4.0	4.03	4.08	4.03	4.06
r , Ohm	10.5	18.3	19.8	17.7	18.1	39.6
ρ_r , Ohm	1484	1500	1491	1500	1491	1497
C' , pF	1427	1530	1725	1766	1725	1725
ρ_a , Ohm	1672	1620	1528	1520	1528	1534
Q_r	141.3	82	75.3	84.7	85.2	37.9
Q_a	159.2	88.3	77.2	85.9	87.4	38.7

The influence of shunting condenser capacity C_0 on equivalent network parameters shows Table 4. Formulae (19) and (20) were used to calculations of equivalent inductance L , anti-resonant frequency f_{a2} , resonant ρ_r and anti-resonant ρ_a wave resistances and according qualities Q_r , Q_a . Resonant f_r and anti-resonant f_{a1} frequencies were measured with loading resistors 3.3 or 335 Ohm and resonant loss resistor r value was determined with approximate formula (16) as follows

$$r = \frac{1}{Y_m} = \frac{(U_{in} - U_R)R}{U_R}. \quad (23)$$

Last two columns of table's data were obtained for $C_0 = 36.1$ nF connecting in series with resistor 21.9 Ohm ($36.1 + R1$) or with that resistor in series with all equivalent network ($36.1 + R2$). A capacity of series condenser C with mica dielectric, measured at 1000 Hz by alternative current bridge, was 1812 pF and it had dielectric loss tangent $\tan \delta = \epsilon_{33m} = 0.0008$. For shunting capacity were used condensers with mica or ceramics dielectric. Inductance L was wound in two insulated wires of 0.5 mm in diameter and its own resistance on direct current measurement was 6.7 Ohm. Different values loss resistor r in table corresponds to various network loading conditions.

It is easy to see, that shunting capacity influence on resonant frequency is very small, but great on anti-resonant frequency. The higher shunting capacity values the lower resonance / anti-resonance range. Calculated quality values for resonance always are less than for anti-resonance. Addition loss resistor in series with shunting capacity decreases both quality factors less than in series with all schemas.

K.Uchino et al [11] in experiments with rectangular piezoceramic plate resonant excitation vibrations shown that quality factor very depends on vibrating velocity level and proposed to include

in electrical equivalent network for high power conditions an addition loss resistor in series with full schema, as I modeled in last row of Table 4. They concluded that there are, of course, different ways to introduce such resistor in equivalent circuit.

The heat generation makes an important role in high power operating piezoelectric devices [9–11]. It is observed in off-resonance frequency under a large electric field applied (1 kV/mm or more) as well as under a relatively small electric field applied (100 V/mm or less) at a resonant frequency. Off-resonance frequency heat provides in a sample volume and dissipated by its surface. The higher ratio of volume / surface the higher sample’s temperature [11]. For resonance case the heat generation is origin in nodal point vicinity where large stress / strains are induced and expansions on full volume. Authors of [10] consider that such phenomenon is caused by mechanic and dielectric loss tangents rises.

5. Results and discussion

As it was shown in previous paragraphs the energy loss in piezoelectric ceramics problems are very complicated and include high power and high frequency dependence [10,11,16] as well as shape dependence.

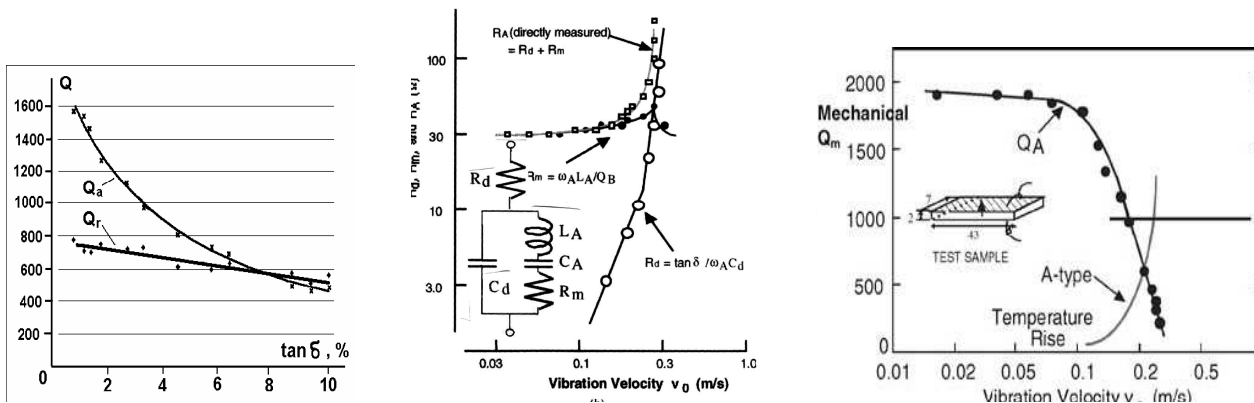


Fig. 5. Quality dependence from dielectric loss tangent or vibration velocity level.

Fig. 5 illustrates the dependence quality from dielectric loss tangent [22] or vibration velocity level [10,11]. Author [22] describes the experimental data presented in left graphs. It shows the dependence of the resonance Q_r and anti-resonance Q_a planar quality factors at the fundamental mode of the disk. The samples were made of a single block $60 \times 60 \times 8$ mm of piezoceramic TsTS-35Y sintered at a non-optimal regime with a large gradient of properties. The samples were polarized in air under pressure at temperature transition through Curie point. At enough equal degree of polarization of the samples the lowering of density, step increase of the static conductivity and increased porosity took place. Under the effect of the indicated factors, the resonance quality factor of planar vibration is reduced a little, but the planar anti-resonance quality factor decreases steeply. Author concludes, that the change of the anti-resonance quality factor Q_a value is a sensitive indicator of the internal active conductivity connected with the internal micro-defectiveness of material structure, such as porosity, not reacted metal components or inclusions, etc. In most cases, the additional firing to $(700 - 900)^\circ C$ of samples with increased static conductivity is enough for essential increasing of the anti-resonance quality factor. These experimental results are in good agreement with restrictive inequalities (2) and show the better dielectric properties the better mechanics and vice versa.

Central graphs of Fig. 5 are created by me on the base of experimental data [11] which were obtained with rectangular piezoelectric plate’s longitudinal vibrations. It demonstrates a vibration velocity dependence of the resistances R_d and R_m in the equivalent electric circuit. Authors make attention on a dramatic change in R_d above a certain threshold vibration velocity. Right graphs show quality dependence upon vibration velocity [10,11]. Both quality factors the resonance Q_r and anti-

resonance Q_a (on Fig its are noted as Q_a , Q_b respectively) sharply decrease after some velocity level is reached.

Equivalent circuit under high power drive for the piezoelectric transducer is represented by a combination of L , C and R . The resonance state has very low impedance. C_d and R_d correspond to the electrostatic capacitance (for a longitudinally clamped sample, not a free sample) and the damped (or “extensive”) dielectric loss $\tan \delta$, respectively, and the components L_A and C_A in a series resonance circuit are related to the piezoelectric motion.

Total resistance $R_A = R_d + R_m$ should correspond to the loss tangent, which is composed of the extensive mechanical losses and dielectric / piezoelectric coupled losses, i.e. to the extensive dielectric and mechanical losses, respectively. Authors [11] introduced an additional resistance R_d to explain a large contribution of the dielectric loss when a vibration velocity is relatively large. The degradation mechanism of the mechanical quality factor Q_m with increasing electric field and vibration velocity is assumed. Fig. 5 shows the change in mechanical Q_m with vibration velocity is almost constant for a small electric field / velocity ratio, but above a certain vibration level Q_m degrades drastically, where temperature rise starts to be observed.

Table 5. Dependence of equivalent network parameters upon sample size (mm²).

Samples, material	50 x 1.3 TBK-3	66.4 x 3.1 TsTBS-3	35.4 x 4.1 TsTS-19	30 x 8 PKD	50 x 1.2 TsTS-19	50 x 1.15 TsTBS-3
C_0 , nF	14 000	18 490	5770	1386	19 000	28 000
f_r , kHz	65.913	31.581	58.929	78.581	41.135	46.224
f_{a1} , kHz	67.917	36.454	69.184	88.820	44.846	52.361
f_{a2} , kHz	67.57	36.62	69.027	96.81	44.76	52.38
C , nF	545	4703	1660	494	2767	5217
L , mHn	10.7	5.48	4.56	8.104	5.42	2.27
r , Ohm	4.45	7.66	19.2	13.5	14	3.3
k_p^2	0.1	0.31	0.32	0.25	0.21	0.34
Q_r	1000	140	86	300	100	200
Q_a	1020	179	98	368	109	226

Authors [11] conclude that R_m , mainly related to the extensive mechanical loss, is insensitive to the vibration velocity, while R_d , related to the extensive dielectric loss, increases significantly around a certain critical vibration velocity. Thus, the resonance loss at a small vibration velocity is mainly determined by the extensive mechanical loss which provides a high mechanical quality factor Q_m , and with increasing vibration velocity, the extensive dielectric loss contribution significantly increases. After R_d exceeds R_m , we started to observe heat generation. All three graphs of Fig. 5 are plotted in principle “as is”, i.e. its not might to explain, why do such phenomena exist? Quality factors and vibration velocity change simultaneously when power supply is rose and both are consequence of a mechanic stress increasing or another reason.

During recent time I studied the radial vibrations a number of piezoelectric disks made from different ceramics and with various thickness / radius ratio. The equivalent R , C , L parameters as well as anti-resonant frequencies were determined with using expressions (21)–(23). Results are presented in Table 5 (notations are same that in Table 4). Its show the higher mechanical quality factor Q the greater equivalent inductance L and the lower equivalent capacity C . Calculated with accounting clamped capacity anti-resonant frequencies f_{a2} are close to measured f_{a1} , excepting thick disk 30×8 mm from PKD material, for which calculated value exceeds measured one in 1.1 time.

To finish this chapter I want to look in the Fig. 6, which demonstrates phase shifts between real / imaginary parts of first and second thin disk radial vibration admittance calculated with formula (13) and determined experimentally with using formula (18).

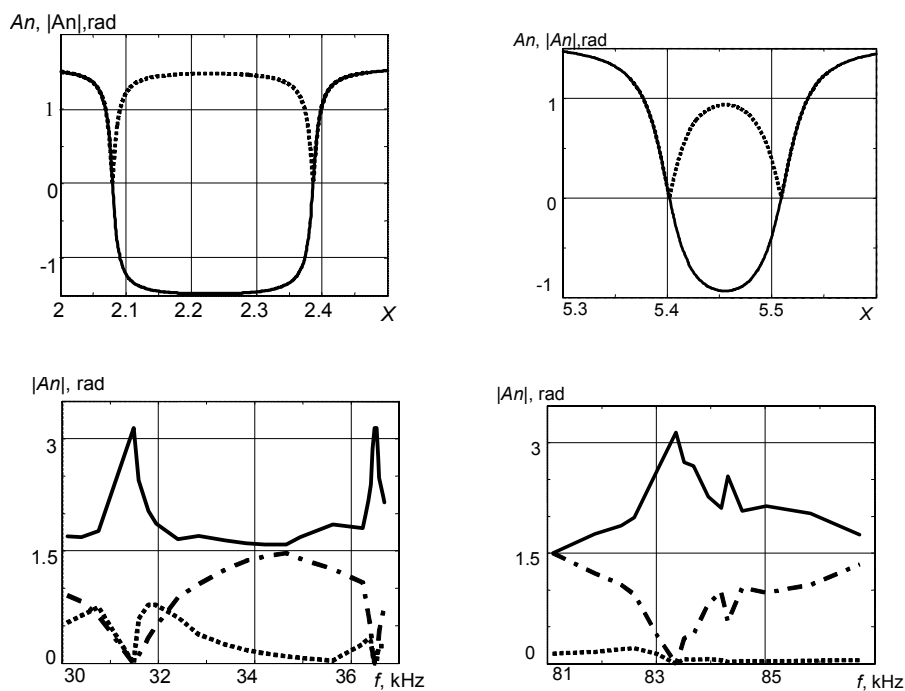


Fig. 6. Calculated and measured phase relations for first two radial resonances.

Both higher graph's two curves were plotted in frequency intervals 2 – 2.5 and 5.3 – 5.6. Symbols $An = v = \text{atan}(w) (w = \text{imag}(Y)/\text{real}(Y))$, unbroken lines) are phase shift's angles and $|An| = \text{abs}(v)$ (broken lines) are modulus of phase shifts. A reason of such plotting is that. Voltmeter measures only effective values of voltage and not sensitive to its polarity. And determined with using cosine law (18) angles of a characteristic triangle are imaged as its modulus. Lower graphs in Fig. 6 represent of phase-frequency relations between sides of this triangle.

A behavior of an angle β near first resonance and antiresonance as well as on second resonance is similar to calculated relations for $|An|$. On the second anti-resonance angles minimum does not rich zero that explains with experimental inaccuracies at small currents measurement.

6. Conclusions

Variants of the known Van-Dyke-type electric equivalent circuit for vibrations of piezoceramic resonators at small and high input power levels as well as those of R, L, C model have been estimated.

The high-power behaviour of piezotransducers is very sensitive to loading conditions and differs for 1) constant voltage, 2) constant current, 3) constant vibration velocity, and 4) constant input power.

The results of Fig. 1 can be explained in the following way. When a piezoceramic piece (specimen) is excited by constant voltage drop, the instantaneous power in the specimen at resonance frequency increases in many times in comparison with the off-resonance case. And when the specimen is excited by constant current, the instantaneous power in the specimen at resonance frequency decreases in the same ratio. Thus, the reason why the admittance curve is non-linear at constant voltage and why it is absent at constant current is a lower level of instantaneous power. Modeling of piezoelectric vibrations by means of R, L, C elements permits us to study these influences on resonant/anti-resonant frequencies as well as on full-conductivities.

Our conception of taking into account only constant (frequency independent) magnitudes of dielectrics, elastic, and piezoelastic loss tangents does not contradict analytical and experimental results. Additional resistor for taking into account high-power conditions influences the resonance to less extent than it does for anti-resonance; and, in my opinion, it must be connected to the equivalent circuit in-

series with the clamped sunit capacitance as it was proposed many years ago by W. Mason for Rochelle salt.

Ten years ago Alex Mezheritsky asked us and himself: “*Elastic, dielectric and piezoelectric losses in piezoceramics: how does it work all together?*”. Now this question may be rewritten as: “*How and why does it work all together?*”.

To answer these and similar questions, further investigations are required very much.

7. Acknowledgements

The author thanks S.P. Timoshenko Institute of Mechanics, Nat. Acad. Sci. of the Ukraine for supports these investigations. He would wish like to acknowledge Prof O.I. Bezverkyh (Ukraine) for useful consultations and Dr A. V. Mezheritsky (USA) for important information.

-
- [1] Cady W. G. Theory of longitudinal vibrations of viscous rods. *Phys. Rev.* **19**, n.1, 1–6 (1922).
 - [2] Van Dyke S. The electric network equivalent of piezoelectric resonators. *Phys. Rev.* **25**, 895(A) (1925).
 - [3] Quimby S. L. On the experimental determination of the viscosity of vibrating solids. *Phys. Rev.* **38**, 568–582 (1925).
 - [4] Dye D. E. The piezoelectric quartz resonator and its equivalent circuit. *Proc. Phys. Soc. (London)*. **38**, 399–453 (1926).
 - [5] Mason W. P. Location of hysteresis phenomena in Rochelle salt. *Phys. Rev.* **58**, 744–756 (1940).
 - [6] Land C. E., Smith G. W., Westgate C. R. The dependence of small-signal parameters of the ferroelectric ceramic resonators upon state of polarization. *IEEE Trans. Sonics and Ultrasonics*. **SU-11**, 8–19 (1964).
 - [7] Martin G. E. Dielectric, elastic and piezoelectric losses in piezoelectric materials. *Ultrasonic Symp. Proc. Milwaukee*. 613–617 (1974).
 - [8] Holland R. Representation of dielectric, elastic and piezoelectric losses by complex coefficients. *IEEE Trans. SU*. **SU-14**, 18–20 (1967).
 - [9] Uchino K., Hirose S. Loss mechanisms in piezoelectrics: how to measure different losses separately. *IEEE Trans UFFC*. **48**, n.1, 307–321 (2001).
 - [10] Ural O., Tunodemi S., Zhuang Yu., Uchino K. Development of a high power piezoelectric Characterization system and its application for resonance/antiresonance mode characterization. *Jpn. J. Appl. Phys.* **48**, 056509 (2009).
 - [11] Uchino K., Zheng J. H., Chen Y. H. et al. Loss mechanisms and high power piezoelectric. *J. Mat. Sci.* **41**, 217–228 (2006).
 - [12] Jaffe B, Cook W. R., Jaffe H. *Piezoelectric ceramics*. Academic Press: London, 1971.
 - [13] Shul’ga N. A., Bolkisev A. M. *The Vibrations of Piezoelectric Bodies*, Nauk. Dumka, Kiev. 1990 (in Russian).
 - [14] Shul’ga M. O., Karlash V. L. *Resonant electromechanic vibrations of piezoelectric plates*. Nauk. Dumka, Kiev. 2008 (in Ukrainian).
 - [15] Karlash V. L. Resonant electromechanical vibrations of piezoelectric plates. *Int. Appl. Mech.* **41**, n.7, 709–747 (2005).
 - [16] Karlash V. L. Energy losses in piezoceramic resonators and its influence on vibrations’ characteristics. *Electronics and communication*. **19**, n.2(a), 82–94 (2013).
 - [17] Karlash V. L. Methods of determine coupling factors and energy losses at piezoceramics resonator’s vibrations. *Acoustic bulletin*. **15**, n.4, 24–38 (2012).
 - [18] Mezheritsky A. V. Electrical measurements of a high-frequency, high-capacitance piezoceramic resonator with resistive electrodes. *IEEE Trans UFFC*. **52**, n.8, 1229–1238 (2005).
 - [19] Karlash V. L. Influence of energy dissipation on amplitude-frequency characteristics of thin piezoceramic disk full conductivity. *Electricity*. N.4, 59–61 (1984) (in Russian).
 - [20] Karlash V. L. Energy dissipation at vibrations of thin piezoceramic circular plates. *Prikl. mekhanika*. – **20**, n.5, 77–82 (1984) (in Russian).

- [21] Mezheritsky A. V. Quality factor of piezoceramics. *Ferroelectrics*. **266**, 277–304 (2002).
- [22] Mezheritsky A. V. Efficiency of excitation of piezoceramic transducer at antiresonance frequency. *IEEE Trans UFFC*. **49**, n.4, 484–494 (2002).
- [23] Mezheritsky A. V. Elastic, dielectric and piezoelectric losses in piezoceramics; how it works all together. *IEEE Trans UFFC*. **51**, n.6, 695–797 (2004).
- [24] Shul'ga M. O., Karlash V. L. Measurement of piezoceramic elements admittance in Meson's four-pole and its variants. *Proc. IV Int. Sci.-Tech. Conf. "Sensors, devices and systems – 2008"*. Cherkasy–Gurzuf. 54–56 (2008) (in Ukrainian).
- [25] Karlash V. L. Planar electroelastic vibrations of piezoceramic rectangular plate and half-disk. *Int. Appl. Mech.* **43**, n.5, 547–553 (2007).
- [26] Gluzman I. A. *Piezoceramics*. Energhiya, Moscow, 1072. 288 p. (in Russian).
- [27] Katz H. W. (ed) *Solid State Magnetic and Piezoelectric Devices*. Willey, New York. 1959.
- [28] US Patent 439 992 1954 / Rosen C. A. 29.06.1954.
- [29] Karlash V. L. Electroelastic vibrations and transformation ratio of a planar piezoceramic transformer. *J. Sound Vib.* **277**, 353–367 (2004).
- [30] Karlash V. Longitudinal and lateral vibrations of a planar piezoceramic transformer. *Jpn. J. Appl. Phys.* **44**, n.4A, 1852–1856 (2005).
- [31] Van der Veen B. The equivalent network of a piezoelectric crystal with divided electrodes. *Phillips Res. Rep.* **11**, 66–79 (1956).
- [32] Munk E. C. The equivalent electrical circuit for radial modes of a piezoelectric ceramic disk with concentric electrodes. *Phillips Res. Rep.* **20**, 170–189 (1965).
- [33] Kalashnikov A. M., Stepuk Ya. V. *Bases of radio-engineering and radiolocation, vibrating systems*. Voeniz, Moscow. 1962. 368 p. (in Russian).
- [34] Zhrebtsov I. P. *Radio-engineering*. Svyaz', Sov. Radio, Moscow. 1965. 656 p. (in Russian).

Моделювання п'єзокерамічних резонаторів з втратами енергії електричними еквівалентними схемами з пасивними елементами

Карлаш В. Л.

*Інститут механіки ім. С. П. Тимошенка НАН України, Київ, Україна
вул. Несторова, 3, Київ, 03057, Україна*

Стаття присвячена аналізу сучасних досягнень в проблемі втрат енергії в п'єзокерамічних резонаторах. Нова експериментальна техніка разом з комп'ютером дозволяє наносити багато параметрів резонатора: адмітанс, імпеданс, фазові кути, компоненти потужності тощо. Подана думка автора, чому добротності на резонансі та антирезонансі різні. Причина полягає у величинах затиснутої ємності та коефіцієнту зв'язку. Чим кращий електромеханічний зв'язок, тим сильніше затиснута ємність і тим більший її вплив на анти-резонансну частоту й добротність. Встановлено також, що значна нелінійність адмітансу в режимі сталої напруги спричинена рівнем миттєвої потужності.

Ключові слова: п'єзокерамічні резонатори, електромеханічний зв'язок, затиснута ємність, миттєва потужність

2000 MSC: 74-05; 74F15

УДК: 534.121.1